Bioorganic Chemistry 43 (2012) 26–36

Contents lists available at SciVerse ScienceDirect

Bioorganic Chemistry

journal homepage: www.elsevier.com/locate/bioorg

Reviews

# Substrate specificity in thiamin diphosphate-dependent decarboxylases

Forest H. Andrews, Michael J. McLeish *

*Department of Chemistry and Chemical Biology, Indiana University–Purdue University Indianapolis, Indianapolis, IN 46202, United States*

ARTICLE INFO

*Article history:*
Received 14 November 2011
Available online 30 December 2011

*Keywords:*
Thiamin-diphosphate
Pyruvate
Benzoylformate
Mutagenesis
Carboligation

ABSTRACT

Thiamin diphosphate (ThDP) is the biologically active form of vitamin $B_1$, and ThDP-dependent enzymes are found in all forms of life. The catalytic mechanism of this family requires the formation of a common intermediate, the 2α-carbanion–enamine, regardless of whether the enzyme is involved in C–C bond formation or breakdown, or even formation of C–N, C–O and C–S bonds. This demands that the enzymes must screen substrates prior to, and/or after, formation of the common intermediate. This review is focused on the group for which the second step is the protonation of the 2α-carbanion, i.e., the ThDP-dependent decarboxylases. Based on kinetic data, sequence/structure alignments and mutagenesis studies the factors involved in substrate specificity have been identified.



**Contents**



## 1. Introduction

Thiamin diphosphate (ThDP, Scheme 1), the biologically active form of vitamin $B_1$, is used as a cofactor by enzymes involved in a wide variety of metabolic pathways [1]. As a consequence, ThDP-dependent enzymes are required to catalyze a diverse range of reactions. In general, these involve the formation and breakdown of carbon–carbon bonds adjacent to a carbonyl group, although the formation of C–N, C–O and C–S bonds is also catalyzed [1].

Unlike, for example, NADH which acts as a cosubstrate, ThDP is a true catalyst and remains bound to the enzyme during the catalytic cycle. In fact, ThDP is able to catalyze many of these reactions in solution, albeit extremely slowly [2]. The first step in that process is formation of the ThDP C2-carbanion or ylide which, subsequently, acts as a nucleophile adding to the α-carbonyl of a 2-keto acid substrate. With the exception of glyoxylate carboligase [3], the active site of a ThDP-dependent enzyme contains a glutamic acid residue which stabilizes the imino tautomer by hydrogen bonding (Scheme 1). C2-deprotonation is further assisted by the cofactor being held in a "V" conformation with the assistance of a bulky hydrophobic residue such as leucine, isoleucine or methionine [4]. In this manner, the imino group is located adjacent to the C2 of the thiazolium ring, thus facilitating proton abstraction (Scheme 1).

ThDP-dependent enzymes have been broadly classified into five families with the largest of these being the decarboxylase family [5]. One member of this family, pyruvate decarboxylase (PDC), may be considered to be the archetypal ThDP-dependent enzyme. The PDC monomer comprises three similarly sized domains: the N-terminal "Pyr" domain which binds the pyrimidine ring of ThDP, a middle domain and the C-terminal "PP" domain which binds the diphosphate (formerly pyrophosphate) moiety. In some enzymes, the middle domain binds a nucleotide ($NADP^+$, FAD or ADP) and it has been suggested that the middle domain was originally

* Corresponding author. Address: Department of Chemistry and Chemical Biology, Indiana University–Purdue University Indianapolis, 402 N. Blackford St., Indianapolis, IN 46202, United States. Fax: +1 317 274 4701.
*E-mail address:* mcleish@iupui.edu (M.J. McLeish).

0045-2068/$ - see front matter © 2011 Elsevier Inc. All rights reserved.
doi:10.1016/j.bioorg.2011.12.001

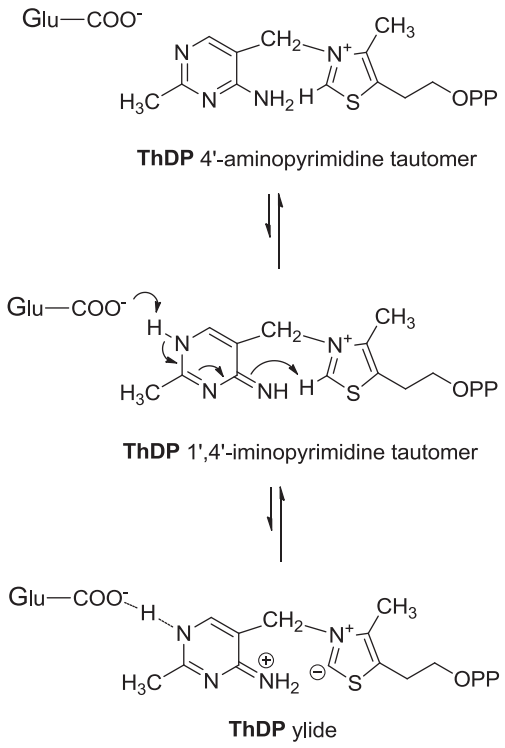


**Scheme 1.** Formation and stabilization of the ThDP ylide.

recruited for that property [5]. The active site is located at the interface between two monomers, with ThDP interacting with the Pyr domain of one monomer and the PP domain of the second. Thus the dimer is the minimal catalytic unit although, like most ThDP-dependent enzymes, PDC exists as a tetramer in its biologically active form. The PDC catalytic cycle is shown in Fig. 1. The first step in catalysis is similar in all enzymes of this type, i.e., the ThDP ylide attacks the carbonyl carbon of the various substrates (in this instance, pyruvate). In addition, all reactions require the formation of the 2α-carbanion–enamine intermediate, sometimes referred to as the "activated aldehyde" [6–8]. In a decarboxylation reaction, the enamine is then protonated, whereas in a carboligation reaction the enamine acts as a nucleophile to an acceptor molecule, such as an aldehyde, 2-keto acid or ketone.

## 2. ThDP-dependent decarboxylases

It has been said that a ThDP-dependent enzyme requires a binding site to overcome entropy problems, a proton relay to assist in the ionization of ThDP and an oxidant to tame the carbanion [2]. Here, using the ThDP-dependent decarboxylases as an example, we will concentrate on the first of these, i.e., the substrate binding site.

### 2.1. "HH-motif" decarboxylases

Besides the glutamic acid residue found in essentially all ThDP-dependent enzymes (Scheme 1), the active site of a large group of ThDP-dependent decarboxylases is characterized by the presence of two histidine residues which are located together on the same polypeptide chain. Hereafter this will be referred to as the "HH-motif". This group includes pyruvate decarboxylases, indolepyruvate decarboxylase (IPDC), phenylpyruvate decarboxylases (PPDCs) and the branched chain 2-keto acid decarboxylase, KdcA. In addition to the two histidine residues, this group possesses a fully conserved aspartic acid residue, as well as a glutamic acid residue which is conserved in all but one instance.

The X-ray structure of pyruvate in complex with the D28A variant of *Saccharomyces cerevisiae* PDC (*Sc*PDC) [9] shows hydrogen bonding between the pyruvate carboxylate and the histidines of the HH-motif, as well as to Glu477 (Fig. 2A). An additional H-bond from the 2-keto group of pyruvate to His115 helps position the substrate for catalysis. A similar array of residues can be seen binding pyruvate in the active site of the *Zymomonas mobilis* enzyme (*Zm*PDC), although, in this instance, only one of the histidines makes a polar contact (Fig. 2B). In the latter case, the use of a tight-binding triazole analogue of ThDP permitted the crystallization of the wild-type (wt) enzyme in the presence of substrate and, as a consequence, the H-bonding between pyruvate and Asp28 can also be observed [10]. Overall, there is broad similarity in the hydrogen bonding networks observed in the structures of *Sc*PDC, *Zm*PDC and *Kluyveromyces lactis* PDC (*Kl*PDC) [9,11] in complex with a variety of ligands. The same residues are observed in the active site of the *Acetobacter pasteurianus* PDC (*Ap*PDC) and, although this structure (PDB ID: 2VBI) is of the holoenzyme, it is virtually superimposable upon that of *Zm*PDC, and it may be expected that ligand binding will also be comparable.

A similar array of ionizable residues is found in other HH-motif decarboxylases (Table 1). Superposition of the active sites of *Zm*PDC and *Enterobacter cloacae* IPDC (*Ec*IPDC), as well as KdcA from *Lactococcus lactis* shows that these four residues occupy nearly identical positions [12–14]. Indeed, the sole exception is provided by the phenylpyruvate decarboxylase from *Azospirillum brasilense* (*Ab*PPDC), in which Glu473 is replaced by a leucine (Leu462) [15]. It has been suggested that Glu473–Asp27–His113 (*Zm*PDC numbering) form a catalytic triad which is involved in the protonation of the enamine intermediate (Fig. 1) [13,16]. In *Ab*PPDC it is proposed that Asp282 could replace the "missing" glutamic acid residue [17].

Some or all of the four ionizable active site residues have undergone mutagenic analysis in *Sc*PDC [18,19], *Zm*PDC [20–23], *Ec*IPDC [13], *S. cerevisiae* PPDC (*Sc*PPDC) [24] and KdcA (McLeish and Stan, unpublished). Consistently, the mutations had a much larger effect on $k_{cat}$ rather than $K_m$ values, providing good indication that those residues played a more prominent role in catalysis than in substrate binding. Taken as a whole, there is high (almost 100%) conservation of the ionizable residues in the HH-motif decarboxylases and, as a result, it is not unreasonable to propose that the binding of the glyoxylate moiety of the various 2-keto acid substrates will be similar in all decarboxylases of this type. Overall substrate specificity will, presumably, be conferred by the other active site residues. To explore this issue in more detail we examined the active sites of PDC, KdcA, IPDC, and PPDC.

The *Sc*PDC (Fig. 2A) and *Kl*PDC [11] structures show that four residues, Phe292, Thr388, Ile476 and Ile480 form a hydrophobic pocket around the methyl group of pyruvate. In the bacterial enzymes (*Zm* and *Ap*PDC) Phe292 has been replaced by a tyrosine residue that forms an additional H-bond with the carbonyl group of pyruvate (Fig. 2B). It should be noted that the yeast enzymes are allosterically activated [9,25] whereas the bacterial enzymes obey Michaelis–Menten kinetics [26,27]. In the allosterically activated PDCs, substrate binding brings about significant conformational changes [9,11,25,28]. To avoid this complication, the structures shown in Fig. 2 are of the activated enzymes, so the interactions are directly comparable.

These "substrate specificity" residues, and their counterparts in other HH-motif decarboxylases of known structure, are shown in Table 2. Residues thought to otherwise influence substrate specificity are also shown in Table 2, while Table 3 provides the kinetic data obtained for a variety of substrates with this group of decarboxylases. The preferred substrates range from pyruvate, through

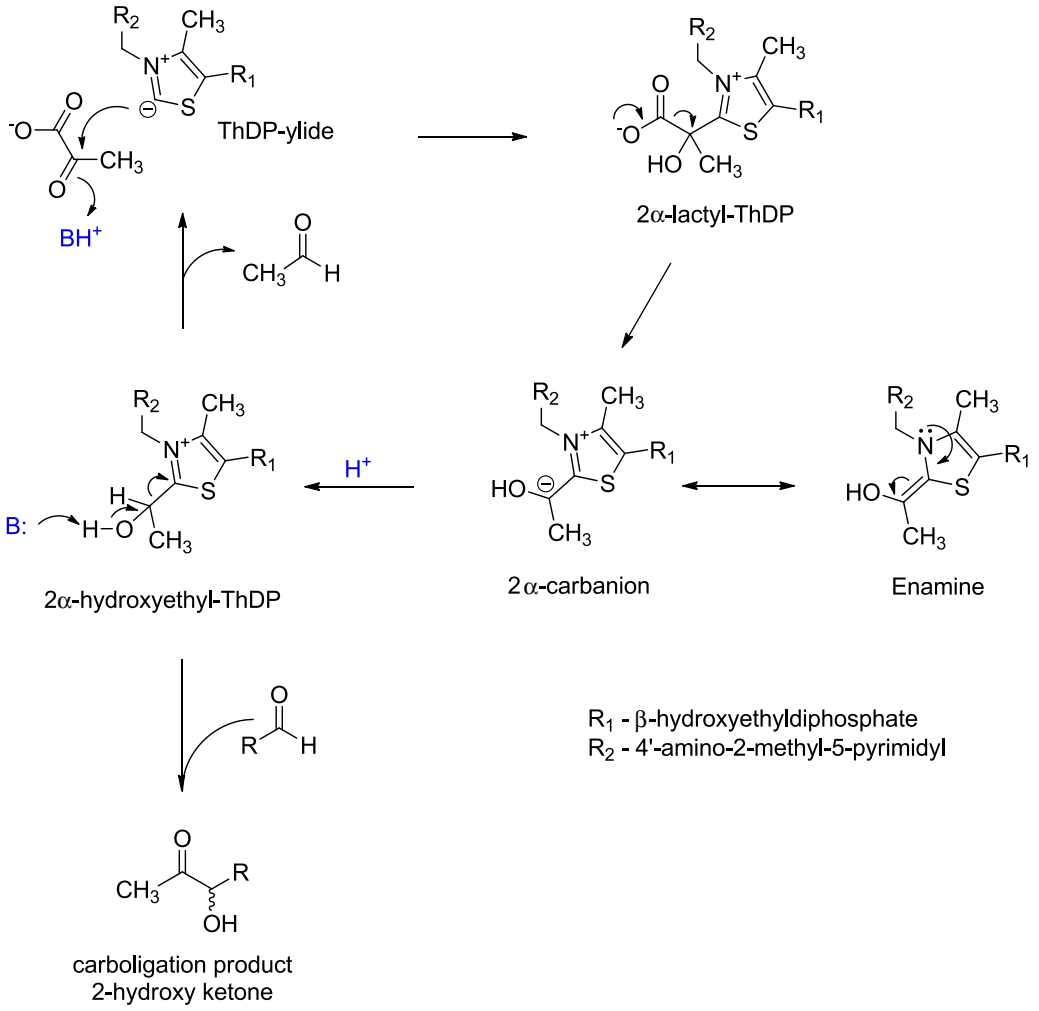


**Fig. 1.** Catalytic mechanism of the archetypal ThDP-dependent enzyme, pyruvate decarboxylase.

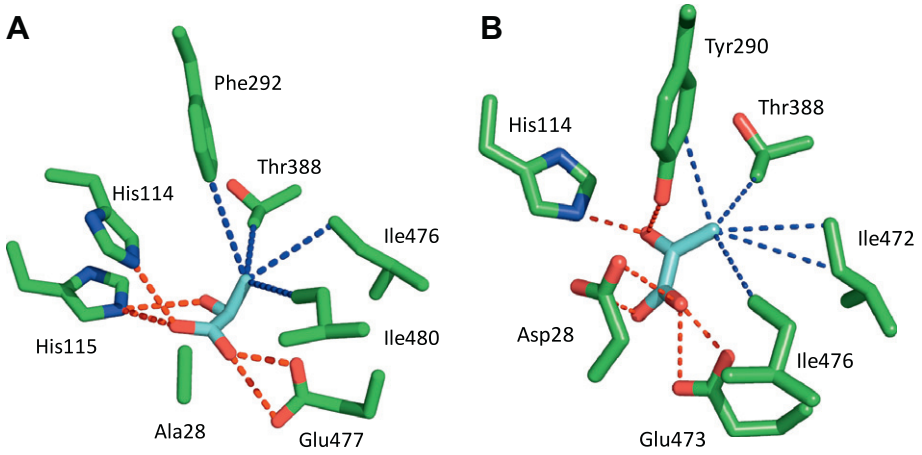


**Fig. 2.** Active site residues of the PDC from (A) *Saccharomyces cerevisiae* and (B) *Zymomonas mobilis*. Hydrogen bonding interactions are shown as red dashes while blue dashes denote van der Waals interactions. For clarity, the cofactor has been omitted. Figures were drawn with PyMOL [77] using data from PDB ID: 2VK1 (*Sc*PDC) and 2WVA (*Zm*PDC).

medium chain 2-keto acids to the appreciably bulkier phenylpyruvate (PPyA) and indolepyruvate (IPyA), and it is instructive to see how the enzymes have dealt with this transition.

One obvious way to accommodate larger substrates is to decrease the size of the residues that are in direct contact with the substrate. In particular, the aromatic residue at position 290 (*Zm*PDC numbering, Table 2), in all cases, has been replaced by a smaller, aliphatic residue. This results in a significant increase in the active site volume. For example, the volume of the *Ec*IPDC active site (130 Å$^3$), in which tyrosine is replaced by threonine, is

**Table 1**
Core ionizable residues of HH-motif decarboxylases.

| Enzyme | | | | |
|---|---|---|---|---|
| *Zm*PDC | Asp28 | His113 | His114 | Glu473 |
| *Sc*PDC | Asp27 | His114 | His115 | Glu477 |
| *Kl*PDC | Asp27 | His114 | His115 | Glu477 |
| *Ab*PPDC | Asp25 | His112 | His113 | – |
| *Ap*PDC[a] | Asp27 | His113 | His114 | Glu469 |
| KdcA[a] | Asp26 | His112 | His113 | Glu462 |
| *Ec*IPDC[a] | Asp29 | His115 | His116 | Glu468 |
| *Sc*PPDC[b] | Asp49 | His144 | His145 | Glu545 |

[a] No ligand present in X-ray structure.
[b] Predicted based on homology model.

more than 50% greater than that of ZmPDC (80 Å$^3$) [12]. In *Ab*PPDC direct interaction with Thr388 has been eliminated, but there are now several new interactions, including those with Ala402, Phe532 and Gln536 (Fig. 3A). KdcA, which has the broadest substrate range (Table 3) also replaces Tyr290 with an aliphatic residue, in this case a serine (Ser286) as well as replacing Ile472 with a valine (Val461). Another modification shown by KdcA is the replacement of Trp392 by phenylalanine (Phe381) which permits access of larger substrates to its active site [14].

In *Ab*PPDC, it is also possible to gauge the effect of a larger substrate. For example, structures have been determined of the enzyme bound to PPyA and to 5-phenyl-2-ketopentanoate acid [17]. Although the latter has two additional methylene units between the phenyl ring and the keto group, there is very little change in active site architecture, and the two substrates are positioned so that the two phenyl rings partially overlap (Fig. 3B). The most significant change to accommodate the larger substrate is the ~2.5 Å movement of Gln536, with smaller (<1 Å) movement being observed for the phenyl rings of Phe465 and Phe532 (Fig. 3B). This was achieved with virtually no change in $k_{cat}/K_m$ value [29]. It would appear that *Ab*PPDC clearly favors aromatic substrates as the $K_m$ value for IPyA is lower than that of PPyA and 40-fold lower than that of the aliphatic, 2-ketohexanoate (Table 3). However, it is not just the presence of a phenyl ring that is important for *Ab*PPDC catalysis. For example, the substrate with only one additional methylene unit, 4-phenyl-2-ketobutanoate, was a significantly worse than both PPyA and 5-phenyl-2-ketopentanoate, showing ~50-fold decrease in $k_{cat}/K_m$ value. Presumably, it is more difficult to achieve the correct positioning of the phenyl ring in the butanoic acid derivative than with the larger, but more flexible, pentanoic acid substrate. The importance of correct substrate alignment is primarily reflected in the $k_{cat}$ values. IPyA and 4-phenyl-2-ketobutanoate, as well as 2-ketohexanoate, all show greatly (20- to 80-fold) reduced $k_{cat}$ values compared to that of the natural substrate [29].

It is also noteworthy that, despite the similarity in residues directly interacting with pyruvate, *Sc*PDC has a much broader substrate range than either *Zm*PDC or *Ap*PDC [27,30]. This has been attributed to replacement of Ala392 in *Sc*PDC by a bulky tryptophan residue in the last two enzymes, a suggestion confirmed by mutagenesis [31]. Further, in *Zm*PDC, *Ap*PDC and *Ec*IPDC, the C-terminal α-helix shields the active site, preventing the entry of larger substrates[12]. In *Sc*PDC this does not occur and, as a consequence, there is no residue structurally equivalent to Trp551.

### 2.2. Benzoylformate decarboxylase

Benzoylformate decarboxylase (BFDC), the penultimate enzyme in the mandelate pathway, catalyzes the nonoxidative decarboxylation of benzoylformate to yield carbon dioxide and benzaldehyde, which enables some microorganisms to utilize *R*-mandelate as their sole carbon source [32–35]. Sequence alignments of BFDC from *Pseudomonas putida* (*Pp*BFDC) showed about 20% sequence identity with the various pyruvate decarboxylases but the HH-motif was missing. Subsequently, the X-ray structure of *Pp*BFDC did reveal the presence of two active site histidine residues [36]. However, although the histidine residues of *Pp*BFDC are positioned similarly to those of the HH-motif enzymes, they are not contiguous, instead being located on each of the monomers that form the active site (Fig. 4).

In addition to that of the unliganded *Pp*BFDC, the structure of its complex with the substrate analogue, *R*-mandelate [37], and of a complex with (*E*)-3-(pyridin-3-yl)acrylaldehyde (PAA), the decarboxylation product of the alternative substrate, (*E*)-2-keto-4(pyridin-3-yl)but-3-enoate, have been solved [38]. Co-crystallization of *Pp*BFDC and the substrate analogue, methyl benzoylphosphonate (MBP), also provided the structure of the stable reaction intermediate analogue, C2α-phosphonomandelyl-ThDP [39]. Taken together these structures provide a wealth of information about the active site of this enzyme.

Besides the glutamic acid residue conserved in nearly all ThDP-dependent enzymes (Glu47), the only ionizable residues in the active site are the two histidines, His70 and His281. Mutagenesis studies support the notion that the two histidine residues, like those in the HH-motif decarboxylases, are involved in catalysis. Alanine variants of His70 and His281 exhibited only moderate changes in $K_m$ values, but $k_{cat}$ values decreased ~4000-fold and 200-fold, respectively, indicating that these residues may act as acid-base catalysts [37,40]. In particular, it was suggested that His70 was likely responsible for stabilization of the first tetrahedral intermediate, as well as deprotonation of the final tetrahedral adduct [36,37]. His281 has been proposed to protonate the enamine intermediate [36,37] essentially carrying out the role of Glu473 in the HH-motif decarboxylases (*vide supra*). The structure of the

**Table 2**
Residues thought to influence substrate specificity of "HH-motif" decarboxylases.[a]

| Enzyme | | | | | | | | | | |
|---|---|---|---|---|---|---|---|---|---|---|
| *Zm*PDC | Tyr290 | Thr388 | Ile472 | Ile476 | Trp392 | Phe393 | | – | Trp551 | Val555 |
| *Sc*PDC | Phe292 | Thr388 | Ile476 | Ile480 | Ala392 | | | | | |
| *Kl*PDC | Phe292 | Thr388 | Ile476 | Ile480 | | | | | | |
| *Ap*PDC[b] | Tyr290 | Thr384 | Ile468 | Ile471 | | | | | | |
| *Ab*PPDC | Thr283 | – | Met461 | Phe465 | Leu384 | | Ala402 | | Phe532 | Gln536 |
| KdcA[c] | Ser286 | Gln377 | Val461 | Ile465 | Phe381 | Phe382 | | | Met538 | Phe542 |
| *Ec*IPDC[b] | Thr290 | Gln383 | Val467 | Ile471 | Ala387 | Phe388 | | Leu538 | Leu542 | Leu546 |
| *Sc*PPDC[d] | Ile335 | Thr444 | Ile544 | Ile548 | Gln448 | | | | Met624 | |

[a] Shaded residues have been shown in X-ray structures to be within 5 Å of substrate.
[b] No ligand present in X-ray structure.
[c] Based on structure containing mimic of reaction intermediate.
[d] Predicted based on homology model.

**Table 3**
Substrate spectrum of "HH motif" decarboxylases.

| Substrate | Parameter[a] | *Sc*PDC | *Zm*PDC | KdcA[d] | *Sc*PPDC[e] | *Ab*PPDC[f] | *Ec*IPDC[g] |
|---|---|---|---|---|---|---|---|
| 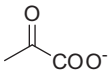 | $K_m$ (mM) | 1.8 ± 0.05[b] | 1.1 ± 0.11[c] | ND | 9.7 ± 0.1 | ND | 3.38 ± 0.18 |
| | $k_{cat}$ ($s^{-1}$) | 37.5 ± 0.32 | 486 ± 49 | ND | 0.34 ± 0.01 | ND | 0.88 ± 0.02 |
| | $k_{cat}/K_m$ | 22 | 440 | 0.085 | 0.035 | 0.012 | 0.25 |
| 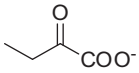 | $K_m$ (mM) | ND | 4.7 ± 0.47[c] | ND | 7.6 ± 0.6 | | |
| | $k_{cat}$ ($s^{-1}$) | 16.9[h] | 320 ± 32 | 14.1[h] | 3.9 ± 0.1 | | |
| | $k_{cat}/K_m$ | ND | 68 | ND | 0.52 | | |
| 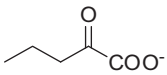 | $K_m$ (mM) | ND | 7.6 ± 0.76[c] | 1.3 ± 0.2 | 2.1 ± 0.1 | | |
| | $k_{cat}$ ($s^{-1}$) | 18.8[h] | 53 ± 5.3 | 9.9 ± 0.4 | 5.2 ± 0.1 | | |
| | $k_{cat}/K_m$ | ND | 7 | 7.8 | 2.5 | | |
| 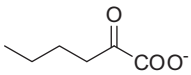 | $K_m$ (mM) | ND | 12.7 ± 1.3[c] | 0.60 ± 0.09 | 0.69 ± 0.01 | 5.5 ± 0.2 | |
| | $k_{cat}$ ($s^{-1}$) | 5.3[h] | 4.0 ± 0.4 | 13 ± 1 | 8.8 ± 0.1 | 17 ± 0.6 | |
| | $k_{cat}/K_m$ | ND | 0.3 | 21 | 13 | 3 | |
| 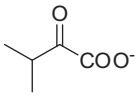 | $K_m$ (mM) | ND | 12.9 ± 0.2[i] | 2.8 ± 0.3 | 8.5 ± 0.4 | | |
| | $k_{cat}$ ($s^{-1}$) | 6.9[h] | 13.7 ± 0.1 | 48 ± 2 | 19 ± 0.5 | | |
| | $k_{cat}/K_m$ | ND | 1.1 | 17 | 2.2 | | |
| 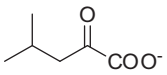 | $K_m$ (mM) | ND | ND | 3.7 ± 0.3 | 0.90 ± 0.03 | | |
| | $k_{cat}$ ($s^{-1}$) | 0.3[h] | 0.3[c] | 49 ± 2 | 10 ± 0.1 | | |
| | $k_{cat}/K_m$ | ND | ND | 13 | 11 | | |
| 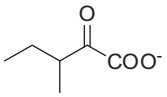 | $K_m$ (mM) | NAD[h] | NAD[c] | 0.76 ± 0.05 | 3.1 ± 0.3 | | |
| | $k_{cat}$ ($s^{-1}$) | | | 41 ± 1 | 11 ± 0.6 | | |
| | $k_{cat}/K_m$ | | | 54 | 3.5 | | |
| 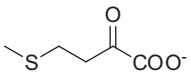 | $K_m$ (mM) | | | 2.4 ± 0.9 | 0.64 ± 0.03 | | |
| | $k_{cat}$ ($s^{-1}$) | | | 8.7 ± 1.3 | 7.7 ± 0.1 | | |
| | $k_{cat}/K_m$ | | | 3.6 | 12 | | |
| 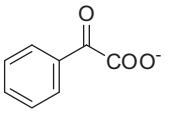 | $K_m$ (mM) | NAD[h] | NAD[c] | 7.5 ± 0.4 | ND | NAD | 1.65 ± 0.03 |
| | $k_{cat}$ ($s^{-1}$) | | | 7.3 ± 0.2 | ND | | 11.6 ± 0.3 |
| | $k_{cat}/K_m$ | | | 0.97 | 0.35 | | 7 |
| 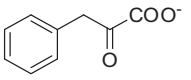 | $K_m$ (mM) | NAD[h] | NAD[c] | 0.21 ± 0.06 | 0.10 ± 0.01 | 1.08 ± 0.09 | |
| | $k_{cat}$ ($s^{-1}$) | | | 27 ± 3 | 20 ± 2.1 | 333 ± 27 | |
| | $k_{cat}/K_m$ | | | 129 | 200 | 309 | |
| 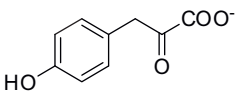 | $K_m$ (mM) | | | 0.63 ± 0.03 | 0.09 ± 0.01 | | |
| | $k_{cat}$ ($s^{-1}$) | | | 2.9 ± 0.1 | 11 ± 0.8 | | |
| | $k_{cat}/K_m$ | | | 4.6 | 125 | | |
| 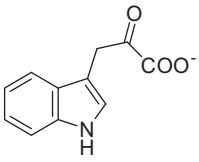 | $K_m$ (mM) | 0.7[g] | NAD[g] | ND | 0.03 ± 0.01 | 0.13 ± 0.01 | 0.02 ± 0.001 |
| | $k_{cat}$ ($s^{-1}$) | 3.81 ± 0.24 | | 1.3[h] | 5.4 ± 0.3 | 4.1 ± 0.1 | 0.98 ± 0.02 |
| | $k_{cat}/K_m$ | 5.4 | | ND | 200 | 32 | 49 |

[a] When using the Hill equation, the parameter $K_m$ is replaced by $S_{0.5}$; ND, not determined, reaction carried out under $V_{max}$ or $k_{cat}/K_m$ conditions; NAD, no activity detected.
[b] Data from [75].
[c] Data from [43].
[d] Data from [62].
[e] Data from [24].
[f] Data from [29].
[g] Data from [76].
[h] Data from [27].
[i] Data from [52].

*R*-mandelate complex also implicates Ser26 in substrate binding (Fig. 4) [37]. The S26A variant was found to have a 25-fold increase in $K_m$ value for benzoylformate, and a 100-fold increase in $K_d$ value for *R*-mandelate, confirming the structural evidence that indicated that this residue likely forms a H-bond with the substrate carboxylate [37,39]. Stopped-flow studies also implicated Ser26 in the later catalytic steps [37], so it was no surprise when subsequent X-ray structures showed that Ser26 also has H-bonding interactions with the C2′ hydroxyl in post-decarboxylation adducts [39].

As with the HH-motif enzymes, the active site of *Pp*BFDC can be nominally be divided into two binding regions: the glyoxylate-binding pocket and the phenyl-binding pocket. Residues forming the glyoxylate-binding pocket include the catalytically important residues, Ser26 and His70, as well as Gly25, Leu110, Ala460, Leu461, and Phe464. Of those, only His70 and Leu110 interact with the carbonyl group, the other residues interact with the carboxylate. The somewhat surprising importance of Leu110 was demonstrated by the alanine variant, which showed a greater than 3 orders of magnitude decrease in specific activity while its $K_m$ value increased by approximately the same amount [8]. The side chain of Leu110 lies within van der Waals distance of the carboxylate group, and it is thought that it might contribute to the strength of the Ser26/carboxylate interaction by restricting movement of the latter [37,39,41]. While no direct interaction is observed for

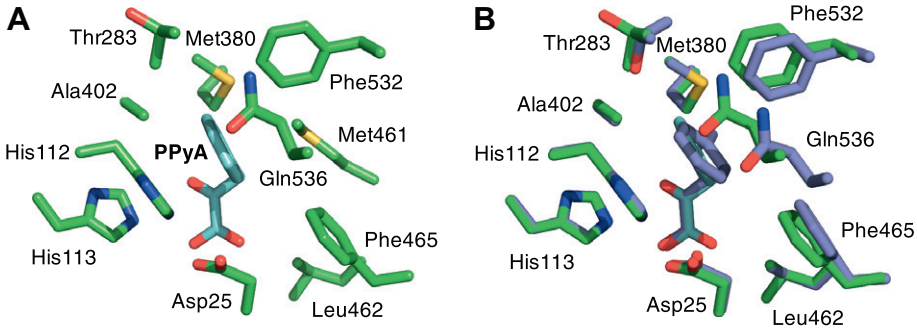


**Fig. 3.** (A) Active site of the phenylpyruvate decarboxylase from *Azospirillum brasilense* (*Ab*PPDC) highlighting residues interacting with phenylpyruvic acid (PPyA). (B) Overlay of the structures of the *Ab*PPDC: PPyA complex (green) and the *Ab*PPDC: 5-phenyl-2-ketopentanoate complex (purple). Data were from PDB ID: 2Q5O and 2Q5Q, respectively. In Fig. 3B, Met461 has been omitted for clarity. (For interpretation of the references to colour in this figure legend, the reader is referred to the web version of this article.)

Gly25 with the carboxylate in any of the X-ray structures, it is notable that Gly25 is within 5 Å of *R*-mandelate and is strictly conserved across all putative BFDC sequences [8,37,42]. This residue is extremely sensitive to mutagenesis [8,42] and it is conceivable that a glycine is required at this position to allow for sufficient flexibility for the proper alignment of the hydroxyl group of Ser26 with the substrate carboxylate [37,39,41]. Both Leu461 and Phe464 are within 4 Å of the carboxylate group of *R*-mandelate, whereas Ala460 is within 5 Å of both the phenyl ring and phosphonomethyl moiety of the MBP-derived adduct, as well as the phenyl ring of *R*-mandelate [37,39,41,42]. Replacement of Ala460 or Leu461 had a variable but modest effect on $K_m$ values. This was accompanied by a ~10-fold decrease in $k_{cat}$ values possibly due to hindrance of product release [43,44]. The remaining glyoxylate-binding residue, Phe464, is one of the few residues shown to adopt multiple rotamers in various *Pp*BFDC crystal structures [36,37,39,41,45]. Site directed [43] and saturation [42] mutagenesis studies have shown that this residue can be replaced without any major impact on enzyme activity.

*Pp*BFDC has a number of residues located within 5 Å of the phenyl ring of MBP or *R*-mandelate which are potentially the principal contributors to the phenyl-binding pocket. These include His281, Thr377, Phe397, Gly401, Leu403, and Phe464. With the exception of His281 and Thr377, the residues are all hydrophobic [36,37]. Even Thr377, which is not hydrophobic, contributes to the overall active site hydrophobicity as the hydroxyl group is rotated in such a way that the β-carbon and γ-carbon atoms of its side chain line the *Si* face of the phenyl ring. In a study conducted by Yep et al., the T377L mutant was generated and found to have close to wt kinetics with benzoylformate as substrate, providing further evidence that only the hydrophobic portion of Thr377 side chain contributes to the phenyl-binding pocket [42]. One of the Leu403 Δ-carbon atoms also lines the face of the phenyl-binding pocket [36] but, this is the residue in *Pp*BFDC that helps maintain the "V" conformation of ThDP necessary for catalytic activity [4]. Gly401 is highly conserved across all ThDP-dependent decarboxylases, and the carbonyl oxygen atom of its backbone is involved in a hydrogen bond with the N4′amino group of the pyrimidine ring of ThDP [36]. Thus Gly401 and Leu403, like the two histidine residues, are probably better ascribed roles in catalysis than in substrate specificity.

The structures of *Pp*BFDC with *R*-mandelate and MBP bound show the side chain of Phe397 to be in an apparent edge to edge interaction with the phenyl ring of the substrate analogues. Analysis of the putative BFDCs in the thiamine diphosphate-dependent enzyme engineering database (TEED) [46] reveals that threonine replaces phenylalanine in the majority of sequences. Thus, this interaction may not be crucial, a suggestion confirmed by the F397A variant which showed little change from wild-type (Horton and McLeish, unpublished).

Another difference between the active site of *Pp*BFDC and that of a HH-motif decarboxylase is that the latter group has a C-terminal α-helix that partially occludes the active site, and which contains several residues involved in substrate recognition. By contrast the active site of *Pp*BFDC is quite open and, for the most part, relatively rigid. Binding of *R*-mandelate, for example, brought about changes in the helix formed by residues 460–470 and very little else with the major change being different rotamers of Phe464 [37]. Regardless of mutagenesis results that indicate that Phe464 could readily be replaced [42], this residue seems to figure prominently in adaptation to substrate binding. Different rotamers were also observed for the MBP-ThDP adduct [39] while the binding of the larger product analogue, PAA, also saw movement of Phe464 but, in this instance, the movement was accompanied by movement of His281 and Phe397 [38]. It should be noted that, in all *Pp*BFDC structures containing bound species, the backbone atoms of the enzymes were virtually superimposable; the substrates were accommodated simply by rotation of side chains (Fig. 4C).

### 2.3. Oxalyl-CoA decarboxylase

Oxalyl-CoA decarboxylase (OXDC) is a homotetrameric ThDP-dependent decarboxylase that catalyzes the nonoxidative decarboxylation of oxalyl-CoA yielding formyl-CoA and carbon dioxide [47]. This allows several bacteria to use oxalic acid, a compound toxic to many organisms, as a source of energy [48]. Like several HH-motif decarboxylases, OXDC possesses an activator binding site [49,50]. However, unlike its PDC counterparts, OXDC is not activated by its substrate, rather it utilizes ADP as an activator [49,51]. While as yet no kinetic analysis of the OXDC substrate spectrum has been published, those residues that apparently bind oxalyl-CoA have been determined through extensive crystallographic studies on OXDC from *Oxalobacter formigenes* (*Of*OXDC) [48,51].

The X-ray structures of *Of*OXDC reveal that, unlike the other decarboxylases discussed in this review, the active site of *Of*OXDC (Fig. 5) lacks the histidine residues postulated to act as acid–base catalysts [48,51]. Rather the side chains of Tyr120 and Glu121 along with the carbonyl oxygen of Ile34 bind a highly ordered water molecule (W1) that is proposed to fulfill the role of His70 in *Pp*BFDC and His114 in *Zm*PDC [23,37,51]. The C-terminus of the holoenzyme structure lacks any interpretable electron density. However, structures with oxalyl-CoA bound show the C-terminus to be ordered as a helix which occludes the active site of *Of*OXDC in a fashion reminiscent of the HH-motif decarboxylase family

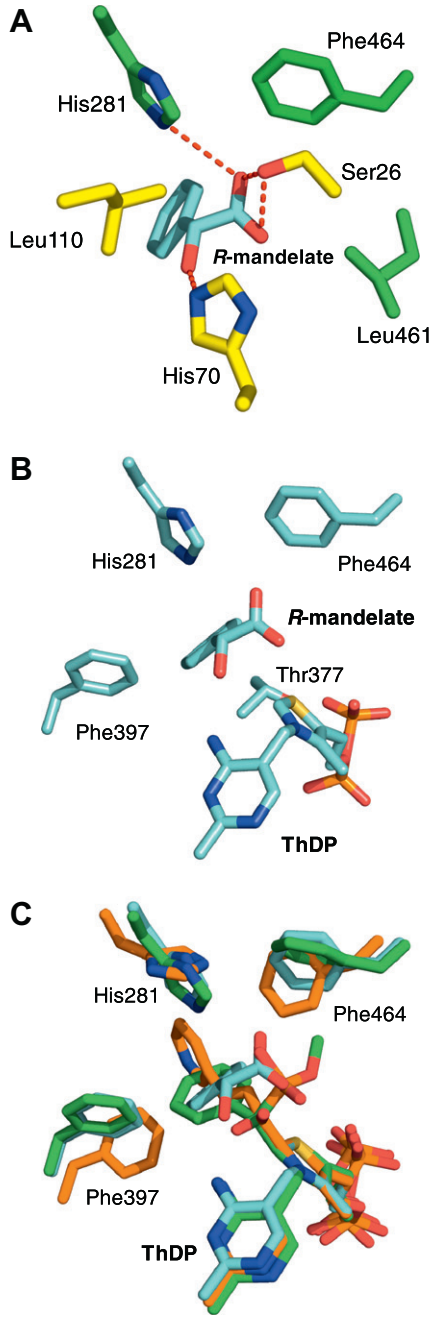


**Fig. 4.** Active site of benzoylformate decarboxylase from *Pseudomonas putida* (*Pp*BFDC) in complex with *R*-mandelate; (A) highlighting histidines from separate monomers and interactions with catalytic residues; (B) showing position of cofactor and residues contributing to recognition of the phenyl ring. (C) Overlay of the *Pp*BFDC: *R*-mandelate (gray), *Pp*BFDC: MBP (green) and *Pp*BFDC: PAA (orange) complexes. Data were from PDB ID: 1MCZ, 3FSJ and 3F6B, respectively. (For interpretation of the references to colour in this figure legend, the reader is referred to the web version of this article.)

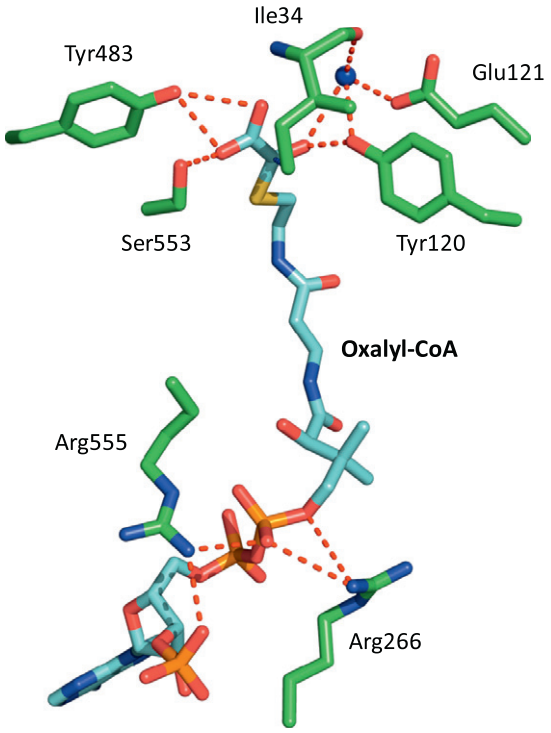


**Fig. 5.** Active site of oxalyl-CoA decarboxylase from *Oxalobacter formigenes* (*Of*OXDC). Data were from PDB ID: 2JI6.

[48,51,52]. This occlusion of the active site by the C-terminus helix allows for the side chains of residues Ser553 and Arg555 to establish interactions with the substrate [51]. Arg555 is positioned in a manner that allows it to form apparent ionic bonds simultaneously with the diphosphate and 3′-phosphate of the CoA moiety [51]. This arginine, along with Arg266, collectively stabilizes the binding of the CoA moiety [51]. The hydroxyl group of Ser553 forms an apparent hydrogen bond with the oxalyl moiety and along with the phenolic hydrogen atoms of Tyr120 and Tyr483, as well as the main chain nitrogen atom of Ile34, creates the oxalyl binding pocket [51]. A truncated *Of*OXDC variant missing both Ser553 and Arg555 was generated and was found unable to perform catalysis, underscoring the significance of the interactions created by the closure of the active site by the C-terminal helix [51]. More recently, the structure of the OXDC from *E. coli* was determined and found to be virtually identical to that of *Of*OXDC [49].

## 3. Carboligation reactions of ThDP-dependent decarboxylases

The reaction pathway of all ThDP-dependent enzymes contains the resonance stabilized 2α-carbanion/enamine ThDP or "active aldehyde" intermediate (Fig. 1). It is the fate of this intermediate that decides the overall activity of an ThDP-dependent enzyme [1]. For example, the decarboxylases favor protonation of the intermediate, and the product is released as the aldehyde. However, in the presence of a second aldehyde, or even if large quantities of product accumulate, C–C bond formation (carboligation) may occur (Fig. 1). Such carboligation reactions provide chiral α-hydroxy ketones which are often used as versatile building blocks, particularly in the pharmaceutical industry [53,54]. Indeed, one of the first examples of an industrially applied biotransformation was the use of fermenting yeast to convert benzaldehyde to *R*-phenyl acetylcarbinol (*R*-PAC), a precursor in the synthesis of 1*R*, 2*S*-ephedrine (Scheme 2) [55,56].

The first step in this sequence is the condensation of benzaldehyde with the "active acetaldehyde" derived from pyruvate, in a reaction catalyzed by *Sc*PDC. It is now known that most of the ThDP-dependent decarboxylases can carry out such carboligation reactions [30,57,58] although the specific activities, enantioselectivity and absolute configuration of the products can vary considerably [27]. Bacterial PDCs, such as *Zm*PDC will carry out the carboligation of two acetaldehyde molecules to produce *S*-acetoin in 20–60% enantiomeric excess (ee). Under the same conditions, *Sc*PDC, KdcA and *Pp*BFDC will produce the *R*-isomer in ~40% ee [27]. A standard test to explore the chemo- and enantioselectivity

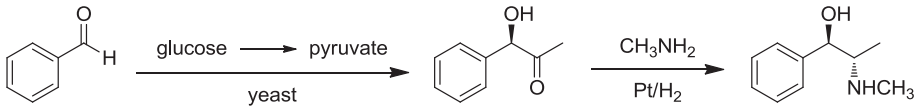


**Scheme 2.** Synthesis of ephedrine.

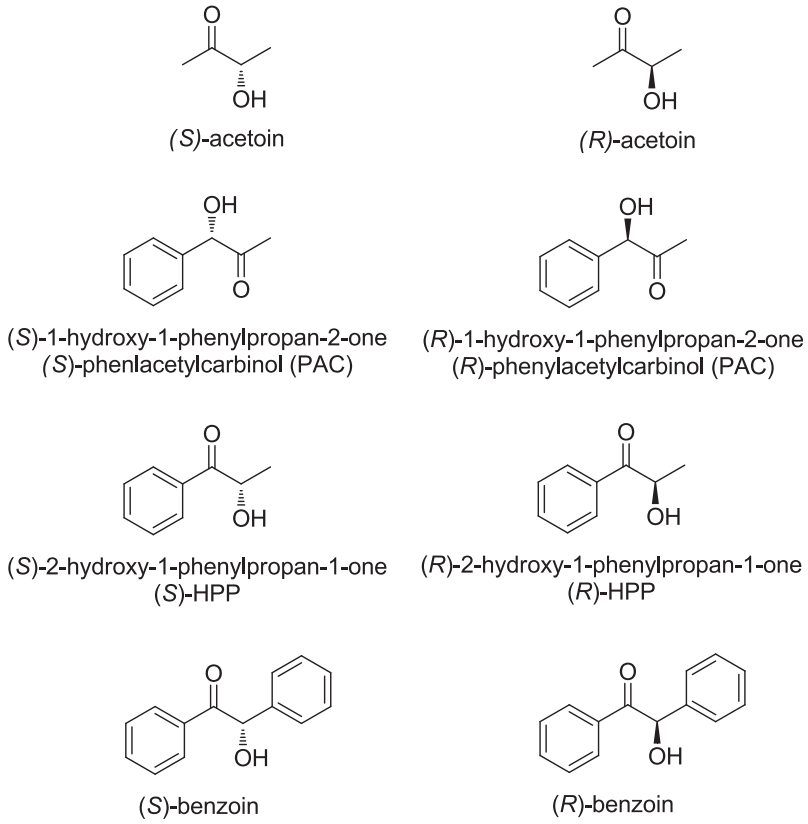


**Fig. 6.** Potential 2-hydroxyketone products from the ThDP-dependent decarboxylase catalyzed carboligation of acetaldehyde and benzaldehyde.

of the various decarboxylases is the mixed carboligation of acetaldehyde and benzaldehyde. This reaction can provide four possible products, each with two possible enantiomers (Fig. 6). The results show that the PDCs are unable to use benzaldehyde as the donor (i.e., the substrate which provides the "active aldehyde") but are readily able to use it as the acceptor forming *R*-PAC. Conversely, *Pp*BFDC prefers benzaldehyde as the donor, producing a mixture of 2-hydroxypropiophenone (2-HPP) and benzoin. Overall there is a good correlation between the range of substrates utilized for decarboxylation reactions and the range of carboligation reactions, with the broad spectrum KdcA providing the most variety [59].

In light of their potential industrial importance, considerable effort has gone into engineering variants of these enzymes with enhanced catalytic properties and extended substrate ranges. In an early study, the W392A variant of *Zm*PDC was engineered to allow easier active site access for aromatic aldehydes, resulting in increased production of *R*-PAC [31]. The I472A variant, prepared to test the importance of Ile472 in stereo-control during carboligation reactions, provided a reduction in the ee of *R*-PAC from 98% to 70% [20]. Most recently, in an important development, it has been shown that replacement of Glu473 with glutamine led to a sizeable reduction in the rate of protonation of the enamine intermediate [16] and greatly enhanced carboligation efficiency [60]. Although wt *Sc*PDC (in the form of whole cells) is commonly used for the production of *R*-PAC, two variants, D28A and E477Q, were able to able to improve the ee from 90–94% to almost enantiopure (>98%) [61]. Given that Glu477 is analogous to *Zm*PDC Glu473, the improvement shown by the *Sc*PDC E477Q variant is easy to interpret in light of recent results [60].

Although KdcA will utilize a wide variety of aldehyde donors and acceptors, its carboligation reaction has not undergone a great deal of mutagenic analysis. In the mixed carboligation assay the wt enzyme produces mixture of *R*-HPP and *R*-PAC in roughly equal amounts [59]. This indicates that both acetaldehyde and benzaldehyde are equally utilized as donor and acceptor. That said, KdcA does show excellent chemoselectivity. For instance, with aliphatic aldehydes larger than acetaldehyde PAC derivatives are formed exclusively, whereas the KdcA-catalyzed reaction of acetaldehyde and 3,5-dicholorobenzaldehyde provides only the 2-HPP derivative [59]. In terms of mutagenesis studies, perhaps the most significant observation to date is that the V461I variant, created in an attempt to convert KdcA into a PDC [62] now provides >98% *R*-PAC (Prühs, Liese and McLeish, unpublished).

*Pp*BFDC is the only known ThDP-dependent decarboxylase that has the innate capability to afford mixed acyloins in the *S*-configuration in high enantiomeric excess [59,63–66]. However, this enantiomer is obtained in high ee only when acetaldehyde is the acyl acceptor. Even slightly larger aldehydes acting as acyl acceptors result predominantly in the *R*-configuration [66,67]. This unique property of *Pp*BFDC is result of an "S pocket" that can only accommodate for the steric bulk of the small acetaldehyde side chain when approaching the planar "activated aldehyde" of the aromatic

donor aldehyde bound to ThDP [8]. Gocke et al. identified residues Pro24, Ala460, and Leu461 as forming this pocket [66], and the roles of these individual residues were assessed by mutagenesis. It was anticipated that each mutant generated would open the "S pocket" of *Pp*BFDC and, hopefully, increase the ee of the *S*-products. Overall, the results suggested that Leu461 is the major contributor in defining the *S*-pocket. In light of these observations, it has been predicted that opening access to *S*-pockets in PDC and KdcA, which are currently blocked by bulky residues, should result in increased formation of *S*-HPP [66]. Certainly, the latter suggestion provided an explanation for the increased production of *S*-HPP observed for the I472A variant of *Zm*PDC [43]. Very recently, it has been shown that the exchange of Glu469 to glycine opens the *S*-pocket in *Ap*PDC for aromatic aldehydes thereby altering stereoselectivity. The E469G variant provides *S*-derivatives with stereoselectivity of up to 89% ee [68].

The recently solved X-ray structure of *Pp*BFDC with (*E*)-3-(pyridin-3-yl)acrylaldehyde (PAA) bound in the active site has shown how the active site is readily able to accommodate substrates larger than benzoylformate [38]. This is consistent with the observation that wt *Pp*BFDC is able to use a variety of meta- and para-substituted benzaldehydes, as well as carbaldehydes, quinolylaldehydes, pyridinylaldehydes, naphthylaldehydes, and even cyclohexane carbaldehyde as acyl donors [69,70]. However, this flexibility did not extend to ortho-substituted acyl donors, a problem that was alleviated by the use of directed evolution. Screening of *Pp*BFDC mutants generated by error-prone PCR identified *Pp*BFDC L476Q and *Pp*BFDC M365L/L461S as variants capable of accepting ortho-substituted aldehydes as acyl donors [71,72].

In many ways H281A is the best characterized of all the *Pp*BFDC variants, having been prepared as a probe of the enzyme's mechanism [37]. Kinetic analysis showed that the substitution considerably reduced the $k_{cat}$ value for benzoylformate decarboxylation reaction, and stopped-flow studies implicated His281 in the protonation of the enamine intermediate [37]. Surprisingly, in addition to accommodating several substituted benzaldehydes as acyl acceptors that wt *Pp*BFDC is unable to use, the H281A variant exhibited an increase in benzoin formation of more than 125-fold [8,70,72,73]. Although the broadened substrate range was not expected, in light of the recent work with the E473Q variant of *Zm*PDC [16,60], the link between the H281A mutation, protonation of the enamine and increased carboligation rate can readily be explained.

## 4. Exchanging substrate specificity in 2-keto acid decarboxylases

As described earlier in this review, considerable effort has been put into determining the role of individual residues in the catalytic mechanism of the various decarboxylases. Additional attention has been focused on expanding the substrate range for carboligation reactions, generally by simply enlarging the active site. However, there has seemingly been less interest in explicitly exploring the factors affecting substrate recognition. This is somewhat surprising in that most of these decarboxylases, certainly the HH-motif enzymes, have the same suite of residues making up the glyoxylate binding site (*vide supra*). Thus, any change in substrate specificity must be brought about by differences in residues contacting the 2-keto acid side chain. Logic would dictate that rational mutation of those residues should bring about predictable changes in substrate spectrum.

Perhaps the first attempt to address this question was carried out by Siegert et al. who, attempted to convert *Zm*PDC into a benzoylformate decarboxylase and, concomitantly, *Pp*BFDC into a pyruvate decarboxylase [43]. Based on comparisons of their X-ray structures, the *Zm*PDC residues, Ile472 and Ile476 were replaced, in turn, by alanine and phenylalanine, respectively. In parallel experiments, the *Pp*BFDC residues, Ala460 and Phe464 were in turn replaced by isoleucine. In terms of generating improved PDC activity the results were disappointing, with none of the *Pp*BFDC variants showing any improvement in $K_m$ value for pyruvate. Although the *Pp*BFDC A460I variant did show a moderate (~15-fold) increase in the value of $k_{cat}/K_m$ for 2-ketohexanoate, the net result of the experiment was the preparation of variants with diminished catalytic activity. The *Zm*PDC variants attained considerably more activity with benzoylformate, at least in relative terms. The wt enzyme has essentially no activity with benzoylformate but the I472A variant exhibited a $K_m$ value of 1.1 mM which is similar to that of the wt enzyme with pyruvate although, at 1.7 $s^{-1}$, the $k_{cat}$ value was still relatively low. By contrast, the $k_{cat}/K_m$ value for 2-ketohexanoate improved by more than five orders of magnitude. Indeed the $k_{cat}/K_m$ value of the I472A variant for 2-ketohexanoate was actually higher than that of wt *Zm*PDC for pyruvate. The I472A/I476A double mutant also showed considerable activity with 2-ketohexanoate but this variant also highlighted the importance of these two isoleucine residues to pyruvate binding as the $K_m$ value increased from 1.1 mM (wt) to 50 mM. [43].

Even though, overall, the active sites of these two enzymes are similar, the positions of the catalytic histidine residues are not identical. So, it was possible that the lack of success in simply replacing residues in *Pp*BFDC or *Zm*PDC with their counterparts in the other enzyme could have been due to differences in binding of the glyoxylate moiety of the substrate. Consequently, it was thought that a study on two HH-motif enzymes would present a better model. As shown in Table 2, the active site of KdcA differs from that of *Zm*PDC by five residues: Ser286, Phe381, Val461, Met538 and Phe542. In an attempt to convert KdcA into a pyruvate decarboxylase, the first four of those residues were replaced, in turn, by their counterparts in *Zm*PDC, Tyr290, Trp392, Ile472 and Trp551, respectively [62]. Once again the results were disappointing. The activity of the wt KdcA with pyruvate can only be measured under $k_{cat}/K_m$ conditions (Table 3) so even being able to measure a $K_m$ value could be considered to be an advance. However, with $K_m$ values between 18 and 65 mM for the single mutants, the improvement was marginal, at best. Attempts at preparing variants with two or three replacements were complicated by stability issues and, regardless, little evidence was found for enhanced PDC activity [62].

The most recent attempt at this "direct swap" approach was carried out on the phenylpyruvate decarboxylase from yeast, *Sc*PPDC [24]. In that study a homology model was used to identify Ile335, Gln448 and Met624 as the residues corresponding to *Zm*PDC Tyr290, Trp392 and Trp551. Replacement of individual active site residues once more provided no appreciable changes in Michaelis–Menten parameters for pyruvate. Moreover, the one stable double mutant that could be isolated had reduced activity with all substrates tested [24]. Nonetheless, the study afforded one intriguing result. This was provided by the E545L variant which was prepared based on the suggestion that having a glutamate or a leucine at this position would decide whether the enzyme was a PPDC or an IPDC [29]. The results showed that binding affinities for PPyA and IPyA were increased and, additionally, the E545L variant now demonstrated substrate activation in both cases. Sadly, this was accompanied by a significant decrease in the $k_{cat}$ value for both substrates and it was difficult to provide any conclusive explanation for the observed changes.

One problem with this rational but relatively simplistic approach is that active sites contain several residues and, in general, these have evolved to bind a preferred substrate. It is unlikely that simply exchanging one residue will provide optimal alignment for

all substrates and intermediates during the catalytic cycle. For example, in the ThDP-dependent enzyme, acetohydroxy acid synthase, it was found that two residues act in concert to mediate substrate specificity and catalytic activity [74]. One way to address this issue is to use saturation mutagenesis on multiple substrate binding residues with the idea of letting nature decide the optimal substitution(s). Such an approach was employed in the latest attempt to convert *Pp*BFDC into a pyruvate decarboxylase [42]. Here twelve non-catalytic residues found within 5 Å of *R*-mandelate [37], and which had structural counterparts in *Zm*PDC, were subjected to saturation mutagenesis. Of these, two variants, T377L and A460Y, were found to have enhanced PDC activity. These were subjected to a second round of mutagenesis and, from both templates, the T377L/A460Y double mutant emerged as having the best PDC activity. While catalytic data for wt *Pp*BFDC with pyruvate can only be obtained under $k_{cat}/K_m$ conditions, the $K_m$ value for the double mutant was found to be 2.0 mM, i.e., similar to that obtained for several wt PDCs [27]. Conversely, at 3.6 $s^{-1}$, the $k_{cat}$ value is still only 3% of wt *Zm*PDC, so there is still room for improvement. Nonetheless, the T377L/A460Y variant was stable and provided a 11,000-fold change in preference for pyruvate over benzoylformate [42]. All in all, this study highlights the benefits of the random, but directed, approach over simply swapping residues.

## 5. Summary

In this review, we have focused specifically on the thiamindiphosphate-dependent decarboxylases. We recognize that there are many other ThDP-dependent enzymes that carry out decarboxylation reactions as part of their overall catalytic mechanism that also deserve similar analysis. However, such enzymes also have a second (or even third) layer of complexity that bears discussion in its own right. We have attempted to draw together data obtained from extensive mutagenic, kinetic, and crystallographic studies of residues involved in substrate recognition in this group of enzymes. Some patterns are obvious, such as replacing a bulky residue with a smaller residue will enable the enzyme to act on a larger substrate. Other changes are not so obvious. For example, both *Pp*BFDC and *Ab*PPDC can accommodate larger substrates simply by small movements in only one or two residues. Unfortunately, this ability is likely to make prediction of substrate specificity a difficult task. Yet it must be done as the TEED database now contains thousands of sequences annotated as ThDP-dependent decarboxylases. At present, it is unclear what exactly these potential enzymes will decarboxylate or, indeed, if they are decarboxylases at all. Hopefully, the daunting task of identifying the reactions catalyzed by these putative decarboxylases will be made simpler as we start to unravel the rules of substrate specificity.

## References


[1] M. Pohl, G.A. Sprenger, M. Müller, Curr. Opin. Biotechnol. 15 (2004) 335–342.
[2] R. Kluger, K. Tittmann, Chem. Rev. 108 (2008) 1797–1833.
[3] A. Kaplun, E. Binshtein, M. Vyazmensky, A. Steinmetz, Z. Barak, D.M. Chipman, K. Tittmann, B. Shaanan, Nat. Chem. Biol. 4 (2008) 113–118.
[4] F. Guo, D. Zhang, A. Kahyaoglu, R.S. Farid, F. Jordan, Biochemistry 37 (1998) 13379–13391.
[5] R.G. Duggleby, Acc. Chem. Res. 39 (2006) 550–557.
[6] A. Schellenberger, Angew. Chem., Int. Ed. 6 (1967) 1024–1035.
[7] R. Kluger, Mechanisms of enzymic carbon–carbon bond formation and cleavage, in: D.S. Sigman (Ed.), The Enzymes, vol. 20, Academic Press, San Diego, 1992, pp. 271–315.
[8] M. Knoll, M. Muller, J. Pleiss, M. Pohl, Chembiochem 7 (2006) 1928–1934.
[9] S. Kutter, M.S. Weiss, G. Wille, R. Golbik, M. Spinka, S. Konig, J. Biol. Chem. 284 (2009) 12136–12144.
[10] X.Y. Pei, K.M. Erixon, B.F. Luisi, F.J. Leeper, Biochemistry 49 (2010) 1727–1736.
[11] S. Kutter, G. Wille, S. Relle, M.S. Weiss, G. Hubner, S. Konig, FEBS J. 273 (2006) 4199–4209.
[12] A. Schütz, T. Sandalova, S. Ricagno, G. Hubner, S. Konig, G. Schneider, Eur. J. Biochem. 270 (2003) 2312–2321.
[13] A. Schütz, R. Golbik, S. Konig, G. Hübner, K. Tittmann, Biochemistry 44 (2005) 6164–6179.
[14] C.L. Berthold, D. Gocke, M.D. Wood, F.J. Leeper, M. Pohl, G. Schneider, Acta Crystallogr. D. Biol. Crystallogr. 63 (2007) 1217–1224.
[15] W. Versées, S. Spaepen, J. Vanderleyden, J. Steyaert, FEBS J. 274 (2007) 2363–2375.
[16] D. Meyer, P. Neumann, C. Parthier, R. Friedemann, N. Nemeria, F. Jordan, K. Tittmann, Biochemistry 49 (2010) 8197–8212.
[17] W. Versées, S. Spaepen, M.D. Wood, F.J. Leeper, J. Vanderleyden, J. Steyaert, J. Biol. Chem. 282 (2007) 35269–35278.
[18] M. Liu, E.A. Sergienko, F. Guo, J. Wang, K. Tittmann, G. Hubner, W. Furey, F. Jordan, Biochemistry 40 (2001) 7355–7368.
[19] E.A. Sergienko, F. Jordan, Biochemistry 40 (2001) 7369–7381.
[20] M. Pohl, P. Siegert, K. Mesch, H. Bruhn, J. Grotzinger, Eur. J. Biochem. 257 (1998) 538–546.
[21] A.K. Chang, P.F. Nixon, R.G. Duggleby, Biochem. J. 339 (1999) 255–260.
[22] Y.G. Wu, A.K. Chang, P.F. Nixon, W. Li, R.G. Duggleby, Eur. J. Biochem. 267 (2000) 6493–6500.
[23] C.Y. Huang, A.K. Chang, P.F. Nixon, R.G. Duggleby, Eur. J. Biochem. 268 (2001) 3558–3565.
[24] M.M. Kneen, R. Stan, A. Yep, R.P. Tyler, C. Saehuan, M.J. McLeish, FEBS J. 278 (2011) 1842–1853.
[25] G. Lu, D. Dobritzsch, S. Baumann, G. Schneider, S. Konig, Eur. J. Biochem. 267 (2000) 861–868.
[26] S. Bringer-Meyer, K.L. Schimz, H. Sahm, Arch. Microbiol. 146 (1986) 105–110.
[27] D. Gocke, T. Graf, H. Brosi, I. Frindi-Wosch, L. Walter, M. Müller, M. Pohl, J. Mol. Catal. B 61 (2009) 30–35.
[28] J.A. Vaccaro, E.J. Crane 3rd, T.K. Harris, M.W. Washabaugh, Biochemistry 34 (1995) 12636–12644.
[29] S. Spaepen, W. Versees, D. Gocke, M. Pohl, J. Steyaert, J. Vanderleyden, J. Bacteriol. 189 (2007) 7626–7633.
[30] H. Iding, P. Siegert, K. Mesch, M. Pohl, Biochim. et Biophys. Acta 1385 (1998) 307–322.
[31] H. Bruhn, M. Pohl, J. Grotzinger, M.-R. Kula, Eur. J. Biochem. 234 (1995) 650–655.
[32] G.D. Hegeman, Meth. Enzymol. 17A (1970) 674–678.
[33] D.N.R. Rao, C.S. Vaidyanathan, Can. J. Microbiol. 23 (1977) 1496–1499.
[34] C.A. Fewson, FEMS Microbiol. Rev. 4 (1988) 85–110.
[35] C. Saehuan, T. Rojanarata, S. Wiyakrutta, M.J. McLeish, V. Meevootisom, Biochim. et Biophys. Acta 1770 (2007) 1585–1592.
[36] M.S. Hasson, A. Muscate, M.J. McLeish, L.S. Polovnikova, J.A. Gerlt, G.L. Kenyon, G.A. Petsko, D. Ringe, Biochemistry 37 (1998) 9918–9930.
[37] E.S. Polovnikova, M.J. McLeish, E.A. Sergienko, J.T. Burgner, N.L. Anderson, A.K. Bera, F. Jordan, G.L. Kenyon, M.S. Hasson, Biochemistry 42 (2003) 1820–1830.
[38] S. Chakraborty, N.S. Nemeria, A. Balakrishnan, G.S. Brandt, M.M. Kneen, A. Yep, M.J. McLeish, G.L. Kenyon, G.A. Petsko, D. Ringe, F. Jordan, Biochemistry 48 (2009) 981–994.
[39] G.S. Brandt, M.M. Kneen, S. Chakraborty, A.T. Baykal, N. Nemeria, A. Yep, D.I. Ruby, G. Petsko, G.L. Kenyon, M.J. McLeish, F. Jordan, D. Ringe, Biochemistry 48 (2009) 3247–3257.
[40] E.A. Sergienko, J. Wang, L. Polovnikova, M.S. Hasson, M.J. McLeish, G.L. Kenyon, F. Jordan, Biochemistry 39 (2000) 13862–13869.
[41] M. Bruning, M. Berheide, D. Meyer, R. Golbik, H. Bartunik, A. Liese, K. Tittmann, Biochemistry 48 (2009) 3258–3268.
[42] A. Yep, M.J. McLeish, Biochemistry 48 (2009) 8387–8395.
[43] P. Siegert, M.J. McLeish, M. Baumann, H. Iding, M.M. Kneen, G.L. Kenyon, M. Pohl, Prot. Eng. Des. Sel. 18 (2005) 345–357.
[44] M. Pohl, D. Gocke, L. Walter, E. Gauchenova, G. Kolter, M. Knoll, C.L. Berthold, G. Schneider, J. Pleiss, M. Müller, Chembiochem 9 (2008) 406–412.
[45] A.K. Bera, L.S. Polovnikova, J. Roestamadji, T.S. Widlanski, G.L. Kenyon, M.J. McLeish, M.S. Hasson, J. Am. Chem. Soc. 129 (2007) 4120–4121.
[46] M. Widmann, R. Radloff, J. Pleiss, BMC Biochem. 11 (2010) 9.
[47] A.L. Baetz, M.J. Allison, J. Bacteriol. 171 (1989) 2605–2608.
[48] C.L. Berthold, P. Moussatche, N.G. Richards, Y. Lindqvist, J. Biol. Chem. 280 (2005) 41645–41654.
[49] T. Werther, A. Zimmer, G. Wille, R. Golbik, M.S. Weiss, S. Konig, FEBS J. 277 (2010) 2628–2640.
[50] X. Zeng, B. Farrenkopf, S. Hohmann, F. Dyda, W. Furey, F. Jordan, Biochemistry 32 (1993) 2704–2709.
[51] C.L. Berthold, C.G. Toyota, P. Moussatche, M.D. Wood, F. Leeper, N.G. Richards, Y. Lindqvist, Structure 15 (2007) 853–861.
[52] A.K. Chang, P.F. Nixon, R.G. Duggleby, Biochemistry 39 (2000) 9430–9437.
[53] C. Fuganti, P. Grasselli, J. Chem. Soc. Chem. Comm. 4 (1982) 205–206.
[54] D. Gala, D.J. DiBenedetto, J.E. Clark, B.L. Murphy, D.P. Schumacher, M. Steinman, Tetrahedron Lett. 37 (1996) 611–614.
[55] C. Neuberg, H. Ohle, Biochem. Z. 128 (1922) 610–615.
[56] G. Hildebrandt, W. Klavehn, Verfahren zur Herstellung von 1-1-Phenyl-2-Methylaminopropan-1-ol., German Patent 548 459, 1932.
[57] M. Pohl, B. Lingen, M. Müller, Chemistry 8 (2002) 5288–5295.
[58] O.P. Ward, A. Singh, Enzyme biotransformation involving α-ketoacid decarboxylases, in: E. Mellado, J.-L. Barredo (Eds.), Microorganisms for Industrial Enzymes and Biocontrol, Research Signpost, Trivandrum, India, 2005, pp. 83–94.
[59] D. Gocke, C.L. Nguyen, M. Pohl, T. Stillger, L. Walter, M. Müller, Adv. Synth. Catal. 349 (2007) 1425–1435.

[60] D. Meyer, L. Walter, G. Kolter, M. Pohl, M. Müller, K. Tittmann, J. Am. Chem. Soc. 133 (2011) 3609–3616.
[61] A. Baykal, S. Chakraborty, A. Dodoo, F. Jordan, Bioorg. Chem. 34 (2006) 380–393.
[62] A. Yep, G.L. Kenyon, M.J. McLeish, Bioorg. Chem. 34 (2006) 325–336.
[63] R. Wilcocks, O.P. Ward, Biotechnol. Bioeng. 39 (1992) 1058–1063.
[64] R. Wilcocks, O.P. Ward, S. Collins, N.J. Dewdney, Y. Hong, E. Prosen, Appl. Environ. Microbiol. 58 (1992) 1699–1704.
[65] A.S. Demir, P. Ayhan, S.B. Sopaci, Water 35 (2007) 406–412.
[66] D. Gocke, L. Walter, E. Gauchenova, G. Kolter, M. Knoll, C.L. Berthold, G. Schneider, J. Pleiss, M. Müller, M. Pohl, Chembiochem 9 (2008) 406–412.
[67] A.S. Demir, T. Dünnwald, H. Iding, M. Pohl, M. Müller, Tetrahdron: Asymmetry 10 (1999) 4769–4774.
[68] D. Rother, G. Kolter, T. Gerhards, C.L. Berthold, E. Gauchenova, M. Knoll, J. Pleiss, M. Müller, G. Schneider, M. Pohl, ChemCatChem 3 (2011) 1587–1596.
[69] T. Dünnwald, A.S. Demir, P. Siegert, M. Pohl, M. Müller, Eur. J. Org. Chem. (2000) 2161–2170.
[70] H. Iding, T. Dünnwald, L. Greiner, A. Liese, M. Müller, P. Siegert, J. Grötzinger, A.S. Demir, M. Pohl, Chem. Eur. J. 6 (2000) 1483–1495.
[71] B. Lingen, J. Grotzinger, D. Kolter, M.R. Kula, M. Pohl, Protein Eng. 15 (2002) 585–593.
[72] B. Lingen, D. Kolter-Jung, P. Dunkelmann, R. Feldmann, J. Grotzinger, M. Pohl, M. Muller, Chembiochem 4 (2003) 721–726.
[73] P. Dünkelmann, D. Kolter-Jung, A. Nitsche, A.S. Demir, P. Siegert, B. Lingen, M. Baumann, M. Pohl, M. Müller, J. Am. Chem. Soc. 124 (2002) 12084–12085.
[74] A. Steinmetz, M. Vyazmensky, D. Meyer, Z.E. Barak, R. Golbik, D.M. Chipman, K. Tittmann, Biochemistry 49 (2010) 5188–5199.
[75] H. Li, F. Jordan, Biochemistry 38 (1999) 10004–10012.
[76] A. Schütz, R. Golbik, K. Tittmann, D.I. Svergun, M.H. Koch, G. Hübner, S. Konig, Eur. J. Biochem. 270 (2003) 2322–2331.
[77] The PyMOL Molecular Graphics System, Schrödinger, LLC.